Eur. Phys. J. Plus (2022) 137:919
https://doi.org/10.1140/epjp/s13360-022-03093-9

THE EUROPEAN PHYSICAL JOURNAL PLUS

Regular Article

Photoionization cross section of a D_2^+ complex in quantum dots: the role of donor atoms configuration

E. B. Al[1], **H. Sari**[2,a], **E. Kasapoglu**[1], **S. Sakiroglu**[3], **I. Sökmen**[3]

[1] Faculty of Science, Physics Department, Sivas Cumhuriyet University, 58140 Sivas, Turkey
[2] Faculty of Education, Department of Mathematics and Natural Science Education, Sivas Cumhuriyet University, 58140 Sivas, Turkey
[3] Faculty of Science, Physics Department, Dokuz Eylul University, 35390 Izmir, Turkey

Received: 3 June 2022 / Accepted: 18 July 2022

Abstract This study reports a theoretical investigation on the electronic spectrum and the photoionization cross section of a singly ionized double donor complex D_2^+ confined in a two-dimensional quantum dot with Gaussian confinement potential. Using the diagonalization method and the effective mass approach, the energy spectrum, binding energy, and photoionization cross section of the D_2^+ complex were obtained for different quantum dot sizes and internuclear distances. The numerical results obtained reveal that the size of the geometric confinement and the configuration of the donor atoms significantly affect the binding energy, equilibrium distance and photoionization cross section of the D_2^+ complex. As a result, the electronic spectrum and optical responses of the artificial molecule D_2^+ complex can be fine-tuned simply by controlling the confinement size and impurity configuration. Also, we conclude that a significant increase in the amplitude of the photoionization cross section is observed when the donor atoms are symmetrically positioned on the x-axes. In addition, the exact convergence of the results obtained in the limiting case to the known results demonstrated the suitability of the method used in this study.

1 Introduction

The tunability of the electronic and optical properties of semiconductor nanomaterials provides significant advantages for the development of novel devices based on these materials. Therefore, researchers remain interested in determining and tuning the electro-optical properties of the low-dimensional semiconductor structures where quantum confinement effects are observed. As it is known, the impurity doping, confinement degree and external fields are frequently used in the process of changing the electro-optical properties of these systems as desired.

In recent years, the adding of a single, magnetic or non-magnetic dopant in low-dimensional semiconductor heterostructures has become technically feasible and opens up significant potential for optoelectronic, photovoltaic and spintronic applications [1–6]. Therefore, investigating the electronic and optical properties of doped semiconductor heterostructures under external fields at different system sizes is important for the design and development of new optoelectronic devices. The evaluation of the singly ionized double donor complex system D_2^+ as a two-level system, especially in the quantum computation process, has gained new insights. The qubit is defined by electron orbital states localized around the different impurity atoms. To give an example, Tsukanov has theoretically investigated the quantum dynamics of an electron bounded in the D_2^+ complex system in a semiconductor host material under the effect of laser pulses and emphasized that this system can be used as a charge qubit where the logical states are defined by the two lowest-lying energy states of the electron localized around one or another donor [7]. Also, Barrett and Milburn have described an applicable scheme for determining the decoherence rate for a charge qubit consisting of an electron shared by a pair of donor impurities in a semiconductor host [8]. They show that by measuring the total probability of a successful qubit rotation as a function of external controllable field parameters, the decoherence rate can be determined. In another notable study, Koiller et al have investigated the electric field manipulation of shallow donor pairs-based charge qubits in *GaAs* and *Si* semiconductors [9]. They conclude that valley interference does not prevent the coherent manipulation of donor-based charge qubits by externally applied electric field for any fixed donor configuration. On the other hand, geometric and dielectric confinement effects on the emission rates, transition energies and charge-density distributions in the lowest-lying energy states of a D_2^+ complex in a spherical quantum dot (QD) have been calculated by Movilla et al within the framework of the effective mass approach [10]. The energy states of spherical QDs with H_2^+-like impurities and the feasibility of their usage as charge qubits were investigated by Kang and coworkers [11, 12]. In these studies, the researchers performed a quantitative analysis of the energy spectrum of the H_2^+-like complex and concluded

I. Sökmen: Retired.

[a] e-mail: sari@cumhuriyet.edu.tr (corresponding author)

Published online: 13 August 2022

that the single ionized double donor system confined in a QD can be considered as a quasi-two-level system and the localized states of this complex may be used as a charge qubit. Recently, the electronic spectrum of the D_2^+ system in two identical coupled, axially symmetrical QDs has been calculated in the presence of the external magnetic field by variational separation of the variables in the adiabatic approach [13]. In this study by Manjarres-García et al, it was noted that the influence of the in-plane confinement on the electron-impurity distance is stronger in spike-shaped QDs and the electronic spectrum dependencies in such structures exhibit a feature similar to that in ring-like structures. Recently, Herhandez et al [14] have performed a detailed work on the magnetic field induced optical absorption coefficients (OACs) of a D_2^+ system confined in a quantum ring. Obtained results indicate that the optical response of the system is strongly dependent on the position of the D_2^+ complex, external magnetic field, hydrostatic pressure, and temperature. Furthermore, the investigations related to the calculations of impurity states [15] and entropy [16] impurities confined in 2D systems have been performed. The obtained results showed that the energy spectrum is strongly dependent on the donor position, thus providing an additional possibility to modify the electronic structure and related optical properties. Recently, the nonlinear optical rectification, the generation of the second and third harmonics of a D_2^+ complex confined in an asymmetric nanowire are theoretically calculated by Giraldo-Tobón et al [17]. The results showed that energy states as a function of the internuclear distance display a molecular-like behavior with the presence of anticrossing points due to the confinement potential provided by the pinch-offs of the V-groove nanowire.

In this regard, it is obvious that the detailed analysis of the electronic structure and optical properties of artificial D_2^+ molecular systems confined in low-dimensional semiconductor heterostructures is an important and current issue. Our aim in this study is to examine the energy levels and photoionization cross section (PCS) of the D_2^+ complex confined in a two-dimensional QD. In the calculation, we will focus on the effect of the QD size and configuration of the D_2^+ complex on the energy spectrum and PCS. Because, as emphasized in previous studies [18–22], the position of the impurity atoms significantly effects on the symmetry of the effective potential in which the electron is confined, and the allowed transitions between energy levels are identified according to the symmetry of the potential. As it is known, the PCS is the process of the electrons bound to a hydrogenic impurity atom by electrostatic interaction to become free with external optical excitation. Therefore, it should depend significantly on the symmetry and size of the effective confinement potential, configuration of the impurity atoms of the D_2^+ complex, as well as on the polarization direction of the external incident optical field. In this study, we consider a Gaussian confinement potential which has proved to be a useful potential in various branches of physics. Bednarek et al. showed that the Gaussian potential (GP) can be studied as a good approximation of confinement potential in electronic QDs [23]. Also, Szafran et al. have shown that the GP is a good approximation for self-assembled QDs [24]. In this context, many studies based on the Gaussian confinement potential have been carried out [25–29]. For instance, Khordad has considered an exciton confined in a spherical QD with the modified GP [25]. On the other hand, the properties of a neutral hydrogenic donor center have been studied for a GaAs semiconductor QD with the Gaussian confinement potential by Boda et al. [26]. Recently, Yahyah et al. have calculated the energy states of shallow donor impurity in GaAs/AlGaAs quantum dot heterostructure with GP have been calculated by the shifted 1/N expansion method [29]. The present calculations show that the donor impurity significantly modifies the electron energy levels of spherical quantum dot and thermal properties.

The article is organized as follows: The general theoretical model of the D_2^+ complex confined in a two-dimensional Gaussian QD and the method used to calculate of the electronic structure is given in Sect. 2. The obtained numerical results of the singly ionized double impurity complex are given in Sect. 3 and we conclude our study in Sect. 4.

2 Theoretical framework

The system considered in this study consists of a singly ionized double donor complex D_2^+ in a two-dimensional QD with Gaussian confinement potential. In the effective mass approximation, for the D_2^+ artificial molecular complex the Schrödinger equation is given as

$$\left[-\frac{\hbar^2}{2m^*}\left(\frac{\partial^2}{\partial x^2}+\frac{\partial^2}{\partial y^2}\right)+V(x,y)+V_C+V_{D_1D_2}\right]\psi(x,y)=E\psi(x,y), \tag{1}$$

where m^* is the electron effective mass, V_C is the electrostatic interaction potential between the electron and donor atoms and $V_{D_1D_2}$ is the repulsive Coulomb potential between donor atoms. The functional form of the Gaussian electron confinement potential is given by

$$V(x,y)=V_0(1-e^{-(x^2+y^2)/R^2}), \tag{2}$$

where R is the effective confinement size defined as the radius of the QD. The positions of the donor atoms are given by the vectors $\mathbf{r}_{D_1}=x_1\hat{x}+y_1\hat{y}$ and $\mathbf{r}_{D_2}=x_2\hat{x}+y_2\hat{y}$. Thus, the separation between the donor atoms defined as the internuclear distance is $D=|\mathbf{r}_{D_2}-\mathbf{r}_{D_1}|$. The attractive interaction potential between the electron and donor atoms is given as:

$$V_C=\sum_{i=1}^{2}\frac{-e^2}{\kappa\sqrt{(x-x_i)^2+(y-y_i)^2}}. \tag{3}$$

The repulsive potential between the donor atoms is written as:

$$V_{D_1D_2} = \frac{e^2}{\kappa\sqrt{(x_1 - x_2)^2 + (y_1 - y_2)^2}}\,. \tag{4}$$

In this study, to examine the effect of the symmetry of the effective confining potential $(V(x, y) + V_C)$ on the electronic spectrum and optical response of the artificial molecule D_2^+, we will consider two different configurations of donor atoms. For example, by adjusting the position of the donor atoms, forbidden optical transitions between energy levels can be made possible by breaking the inversion symmetry. By denoting impurity atoms 1 and 2 with D_1 and D_2, respectively, the position of the first donor atom in both cases will be taken as: D_1 $(x_1, y_1 = 0)$. The position of the second donor atom will be as follows: Case I: $D_2(x_2 = y_2 = 0)$ and accordingly, $D = |x_1|$. Case II: $D_2(x_2 = -x_1, y_2 = 0)$ and accordingly, the internuclear distance is $D = 2|x_1|$. The bound energy states of the D_2^+ complex confined in a 2DQD can be obtained by solving Eq. 1 using the 2D diagonalization technique [30, 31].

At this stage, we would like to give theoretical information about the PCS, which is important for the single ionized double impurity system characterization. As is known, the PCS is defined as the optical transition from the ground state (initial state) of the QD with impurity to the first allowed impurity-free excited state (final state). The initial (final) state is described by ψ_i (ψ_f) and E_i (E_f). The PCS, starting from Fermi's golden rule in the dipole and effective mass approximation, is given by [18, 21, 32, 33]

$$\sigma(\hbar\omega) = \left[\left(\frac{F_{eff}}{F_0}\right)^2 \frac{n_r}{\kappa}\right] \frac{4\pi^2}{3}\beta_{FS}\hbar\omega \sum_f |\langle\psi_i|\mathbf{r}|\psi_f\rangle|^2 \delta(E_f - E_i - \hbar\omega)\,, \tag{5}$$

where n_r is the refractive index of the semiconductor, κ is the dielectric constant of the medium, β_{FS} is the fine structure constant and $\hbar\omega$ is the photon energy. F_{eff} is the effective electric field of the incident photon and F_0 is the average electric field in the medium. In general, since the shape of the PCS is not affected by the effective field ratio, F_{eff}/F_0 is taken as approximately unity [20, 34–36]. $\langle\psi_i|\mathbf{r}|\psi_f\rangle$ is the dipole position matrix element between the initial-ψ_i and final-ψ_f states. In general, in the calculation of the PCS the δ-function is replaced by a narrow Lorentzian function [19, 37, 38]

$$\delta(E_f - E_i - \hbar\omega) = \frac{\hbar\Gamma}{\pi[(\hbar\omega - (E_f - E_i))^2 + (\hbar\Gamma)^2]}\,, \tag{6}$$

where Γ is the hydrogenic impurity linewidth. It is worth mentioning that in the calculation of the PCS in the 2DQD structure the incident radiation will be chosen with xy-plane component. It should also be noted that the final state wave function of the first allowed dipole transition ψ_f depends on the position of the impurity atoms in the xy-plane and the polarization of the incident radiation. For x-polarization, an optical transition from the ground state of the QD with impurity to the ground state without impurity is allowed in case I. Whereas in case II the optical transition from the ground state with impurity to the first excited impurity-free state is allowed.

3 Results and discussion

Using the two-dimensional diagonalization method and within the framework of the effective mass approach, the electronic spectrum for the D_2^+ complex confined in a 2DQD with Gaussian confinement potential was calculated. In our numerical calculations, we used the following physical parameters, which are commonly used for *GaAs/GaAlAs* semiconductor materials [21, 32]: $m^* = 0.067m_0$, $\kappa = 13.18$, $\Gamma = 0.1\ meV$, $V_0 = 228\ meV$, $T_{ij} = 0.14\ ps$, $\mu = 4\pi \times 10^{-7}\ H/m$, $n_r = 3.2$ and $\sigma_s = 1 \times 10^{23}\ m^{-3}$.

In Fig. 1, we present the change of the total energy of the D_2^+ complex corresponding to first six energy states as a function of the internuclear distance-D for three different values of the parameter-R, in case I. In this case, one of the atoms (D_2) is fixed in the center of QD and the other (D_1) moves to the right on the x-axis, i.e., D_1 $(x_1, y_1 = 0)$ and D_2 $(x_2 = 0, y_2 = 0)$. In general, the variation of the low-lying energy states with the internuclear distance-D appears similar to that of the hydrogen molecule-ion H_2^+ [17, 39–42]. As seen in this figure, when the impurity atoms are very close to each other, the first and third excited energy states are degenerate doubly since the effective potential $(V(x, y) + V_C)$ is almost circularly symmetrical. On the other hand, as the first impurity atom (denoted by D_1) moves away from the center to the right, the circularly symmetrical structure of the effective potential begins to break down and the degenerate energy levels split into two. Even more remarkably, when the first impurity atom is moved sufficiently far to the right, the electron remains mainly in the attraction field of the second impurity atom (D_2) fixed at the center of the QD, and the effective potential energy function gains symmetrical character again. As clearly seen in Fig. 1a and b, the energy levels that split in two, (E_2, E_3) and (E_5, E_6) pairs, with the effect of this transformation they revert to a twofold degenerate state again. In large-sized QDs, it is seen that the system becomes symmetrical again at a larger internuclear distance value. For example, while the first excited state becomes degenerate again at approximately $D = 15\ nm$ for $R = 10\ nm$, this value is around $D = 18\ nm$ for $R = 20\ nm$. However, from Fig. 1c, it is seen that the internuclear distance value at which this transformation observed is greater than $20\ nm$ for $R = 50\ nm$. It should also be noted that as the effective QD size-R is reduced, an upward shift in total energy is observed as the position of the equilibrium distance shifts toward smaller values, which is expected due to a higher confining capacity of the QD. For example, the equilibrium distance is approximately $\sim 3\ nm$ for $R = 10\ nm$ and

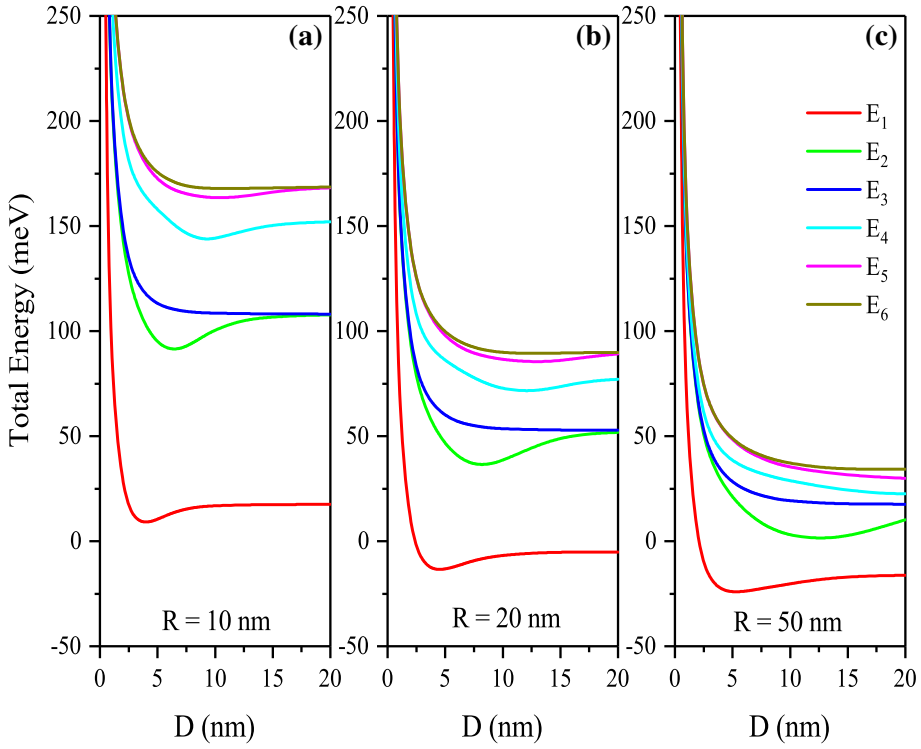

Fig. 1 Evolution of the total energy of the D_2^+ complex corresponding to the first six states as a function of internuclear distance for (**a**) $R = 10\ nm$, (**b**) $R = 20\ nm$ and (**c**) $R = 50\ nm$ for the case where one of the donor atoms is placed in the center of the QD

$\sim 5\ nm$ for $R = 50\ nm$. This feature is qualitatively in agreement with the results obtained for the H_2^+ molecular ion [39]. On the other hand, the dissociation energy, defined as the energy difference between the asymptotic energy for sufficiently large internuclear distance ($D \to \infty$) and the total energy minimum, decreases as the geometric confinement weakens. The physical reason for this behavior is that the artificial molecular complex is more stable in the range where the geometric confinement is strong. It should be emphasized that, as expected, total energies of the D_2^+ complex tend asymptotically to those of the D^0 system (single donor atom with an electron) positioned at the center of the 2DQD for sufficiently large internuclear distance values [43]. This compatibility is particularly evident at relatively narrow QDs. If we give a comparison, for $R = 20\ nm$, the ground and first excited state energies of D^0 are $E_1 = -5.86\ meV$ and $E_2 = 52.71\ meV$ [43]. These energies of the D_2^+ complex converge to $E_1 = -5.15\ meV$ and $E_2 = 51.87\ meV$ at large internuclear distances for $R = 20\ nm$.

In Fig. 2, we show the total energy variation of the D_2^+ complex with the configuration of the donor atoms defined in case II as a function of the internuclear distance for different values of the QD size. In this case ($y_1 = y_2 = 0$, $x_1 = -x_2$), both donor atoms are positioned symmetrically about the y-axis on the x-axis. From Fig. 2 one can observe that as in the previous case, when the donor atoms are very close together, the system has circular symmetry and there are doubly degenerate levels in the energy spectrum. With the increase of the distance between atoms, the circular symmetry is broken and as a result, the degeneration seen in the energy spectrum disappears. In the region where the internuclear distance is large enough, the electrostatic interaction between the donor atoms and the electron weakens and the system turns into a single electron confined in a 2DQD with circular symmetric potential resulting in doubly degenerate energy levels. In order to compare our results, we also calculated the energy levels of a single electron confined in the 2DQD with Gaussian potential. As can be clearly seen in Fig. 2, the solid lines corresponding to the D_2^+ complex energies converge asymptotically to single electron energies (dashed straight lines) for sufficiently large internuclear distance values. To illustrate this effect clearly, in this case we increase the distance between the donor atoms up to 100 nm. This compatibility in the limit case confirms the suitability of the method used in the study.

Figures 3 and 4 show the binding energies versus the QD size trend for three different values of internuclear distance in cases I and II, respectively. Obviously, with the increase of the internuclear distance, a reduction is observed in the binding energy corresponding to all the energy levels considered for both cases. In general, we observe that for a constant internuclear distance, with increasing QD size, the binding energy peaks in both cases, then decreases and converges to a certain value. Similar to the behavior of the total energy with the internuclear distance-D, the binding energy is also split into two by the degeneration of the energy levels. As can be seen from Figs. 3 and 4, the internuclear distance-D induces a significant change in the magnitude of the binding energies. Such that the order of binding energies varies at large D values depending on the distribution of the wave function corresponding to the energy level of interest. For example, as seen in Fig. 4c, for $D = 10\ nm$ in the region $R > 40\ nm$, the binding energy corresponding

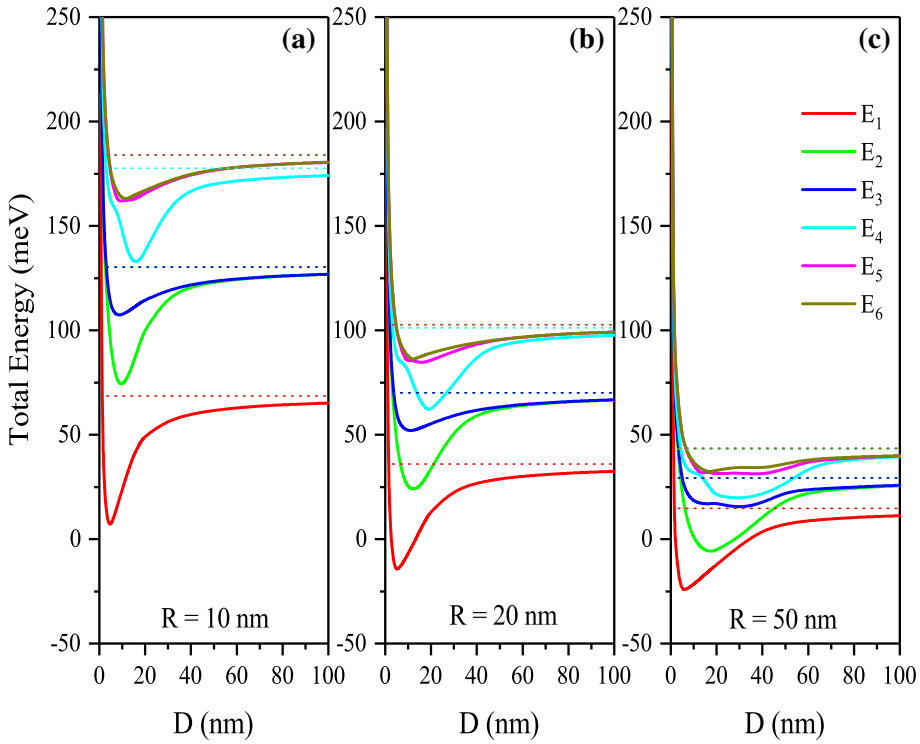

Fig. 2 Evolution of the total energy of the D_2^+ complex corresponding to the first six states as a function of internuclear distance for (**a**) $R = 10\ nm$, (**b**) $R = 20\ nm$ and (**c**) $R = 50\ nm$ for the case where the donor atoms are placed symmetrically on the x-axis. Dashed lines indicate single-electron energy levels

to the first excited state is the largest one. Whereas, in other cases where the donor atoms are closer together ($D = 1, 5\ nm$), the binding energy corresponding to the ground state is the largest.

Before concluding this section, it is worth pointing out that in case I where one of the donor atoms is fixed to the center of the system, the binding energies of the D_2^+ complex converge to those of the single donor impurity atom (D^0) located at the center of the QD for sufficiently large internuclear distance values. This feature may be better recognized from the internuclear distance dependence of the D_2^+ binding energy. To illustrate this feature clearly, we also calculated the binding energies of the single donor atom confined in the 2DQD for selected values of QD sizes, $R = 10$ and $20\ nm$. In Fig. 5, the variation of the binding energies corresponding to the first four energy states are given as a function of the internuclear distance-D for two different R values. It can be seen from this figure that the binding energies corresponding to E_1 and E_3 decrease rapidly with the internuclear distance and then converge to that of the single impurity atom. However, it is seen that the binding energies corresponding to the E_2 and E_4 levels exhibit different behavior when the donor atoms are very close to each other, and as the distance between the donor atoms increases, they converge to the relevant energy values of the single donor impurity. The physical origin of this different behavior is due to the electron probability density corresponding to the E_2 and E_4 levels. To further elaborate Fig. 5, the probability density functions corresponding to the first four states are given in Fig. 6. As seen from Fig. 6, since the probability density of the ground state $|\psi_1|^2$ has circular symmetry and a central vertex, when the donor atom represented by D_1 is moved to the right on the x-axis, its electrostatic interaction with the electron weakens and causes a decrease in the binding energy. On the other hand, the probability distribution corresponding to the first excited state $|\psi_2|^2$ has two peaks symmetrical about the y-axis and its amplitude is zero at the origin. Therefore, when the D_1 donor atom moves away from the center to the right on the x-axis, the electrostatic interaction between the electron and the D_1 donor atom first increases to a maximum, then begins to decrease. Whereas the electron probability distribution corresponding to the second excited state $|\psi_3|^2$ has two symmetrical peaks about the x-axis and its amplitude is zero at the origin. Therefore, as can be seen in Fig. 6, the binding energy corresponding to the E_3 level decreases monotonically with the D parameter and converges to a constant value. By a similar analysis for the electron probability corresponding to the E_4 level $|\psi_4|^2$, we can deduce that when the D_1 donor atom is moved to the right, depending on the probability distribution the binding energy corresponding to this level will first decrease, then increase to a maximum value, and then decrease and converge to a certain value. Another important point to be emphasized here is that the variation of binding energies as a function of the internuclear distance-D is similar to the projection of electron probability distributions corresponding to the relevant energy states.

Finally, let us discuss the effects of QD size and internuclear distance on the PCS of the single-ionized double-donor complex D_2^+. In the first step, we will present the effect of QD size and internuclear distance on the threshold energy and amplitude of the PCS peak, in case I. As mentioned earlier, optical transition from the ground state of the D_2^+ complex (initial state) to the non-correlated

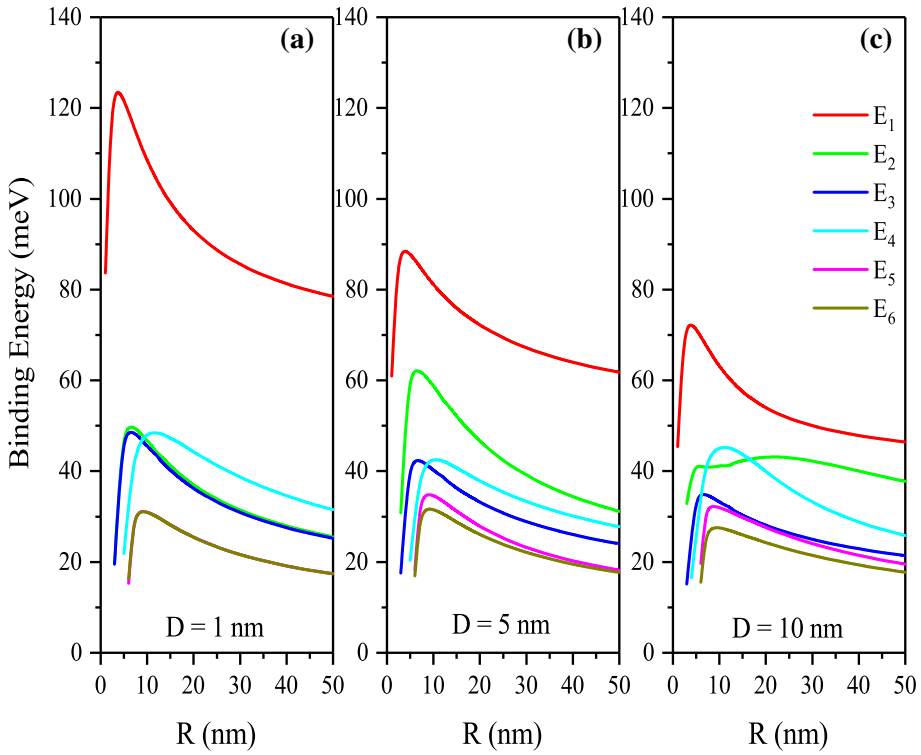

Fig. 3 Variation of the binding energy of the D_2^+ complex corresponding to the first six states as a function of the QD size for (**a**) $D = 1\ nm$, (**b**) $D = 5\ nm$ and (**c**) $D = 10\ nm$ for the case where one of the donor atoms is placed in the center of the QD

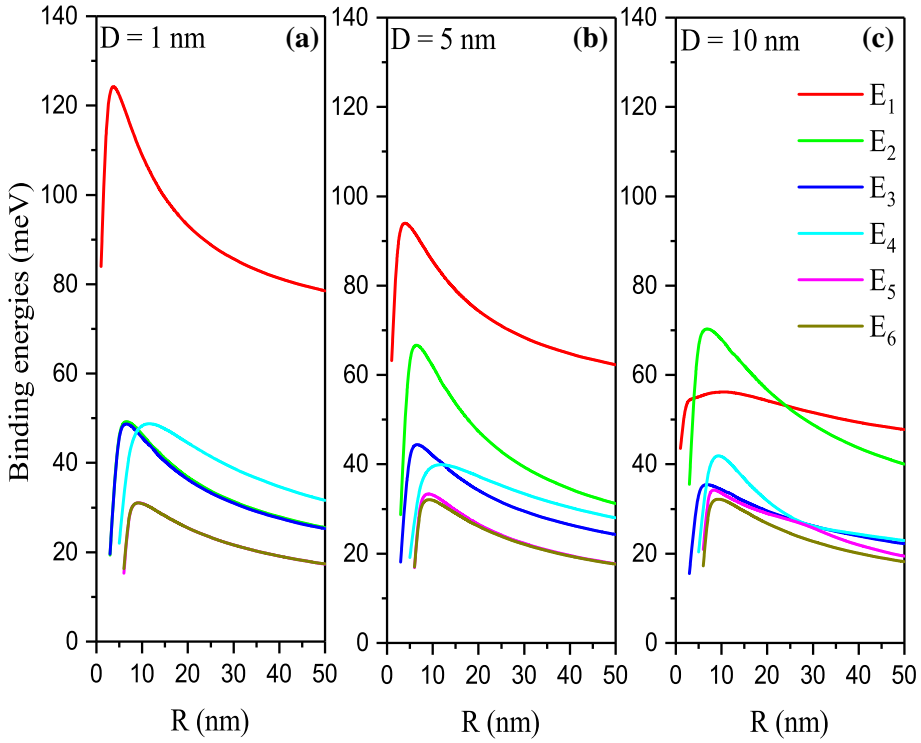

Fig. 4 Variation of the binding energy of the D_2^+ complex corresponding to the first six states as a function of the QD size for (**a**) $D = 1\ nm$, (**b**) $D = 5\ nm$, and (**c**) $D = 10\ nm$, for the case where the donor atoms are placed symmetrically on the x-axis

electron ground state (final state) is allowed for x-polarized incident radiation. In Fig. 7, the PCS dependence on the QD size is given as a function of the incident electromagnetic radiation for a fixed value of the internuclear distance, $D = 1\ nm$. From this figure it can be observed that as the QD size increases, the peak magnitude increases and its position shifts to lower photon energies. As seen in

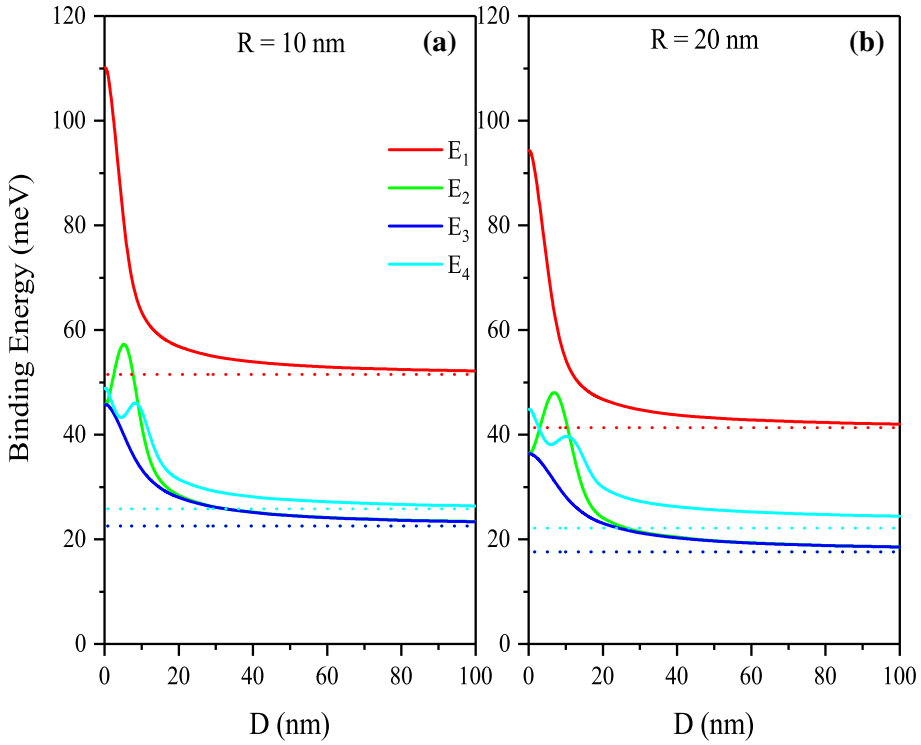

Fig. 5 Evolution of the binding energy corresponding to the first four states as a function of the internuclear distance for (**a**) $R = 10\ nm$, (**b**) $R = 20\ nm$, for the case where one of the donor atoms is centrally located. Dashed lines indicate related binding energies of the single-donor impurity (D^0) located at the center of the QD

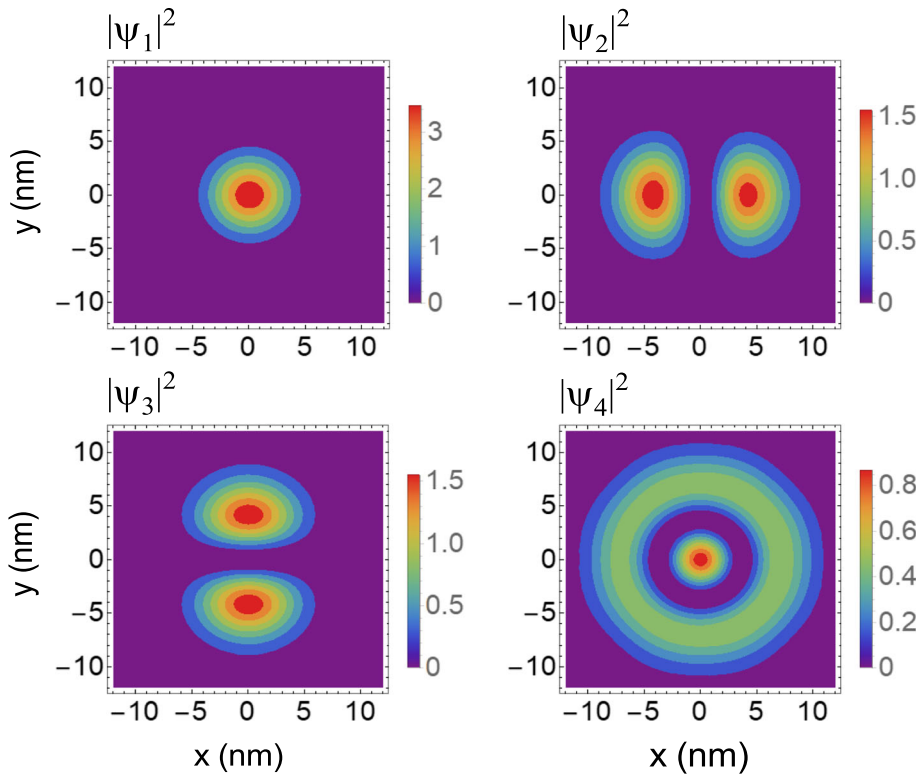

Fig. 6 Contour plot of the probability density for the first four states of the D_2^+ complex confined in the QD for $D = 2\ nm$ and $R = 10\ nm$. Results for the case where one of the donor atoms is placed in the center of the QD

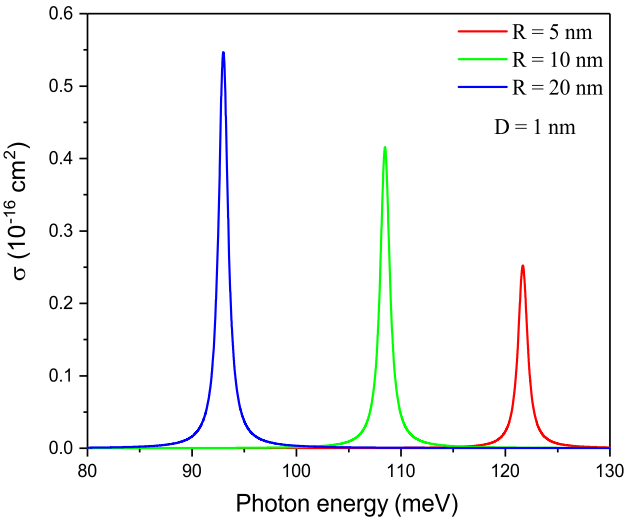

Fig. 7 PCS of the D_2^+ complex as a function of the incident photon energy for $R = 5$, 10, and 20 nm when $D = 1$ nm. Results for the case where one of the donor atoms is placed in the center of the QD

Eq. 6, the resonance peak of the PCS is obtained when the photon energy is equal to the binding energy ($\hbar\omega = E_f - E_i = E_B$). The physical reason for the redshift observed in the peak position is that the binding energy decreases with the QD size, as mentioned in the previous discussions. On the other hand, the reason for the reduction in the peak amplitude with the decrease of the R parameter can be explained as: The probability of the correlated and the non-correlated electronic wave functions to be localized in the same plane increases in the regime where the geometric confinement is strong, and as a result, a significant decrease in the matrix element occurs.

To illustrate the effect of internuclear distance on the PCS of the D_2^+ complex, we present the variation of PCS as a function of photon energy for three different values of the R and D parameters in Fig. 8. Examining the curves in this figure it is seen that the peak position of the PCS moves toward lower photon energies and its amplitude increases with increasing R values for all D values considered. However, the variation of PCS amplitude with internuclear distance does not exhibit a monotonous behavior. As can be seen in Fig. 8, the peak amplitude first increases with the increase of the internuclear distance and decreases at larger distances. This behavior can be explained in detail from the fact that the peak amplitude of PCS is proportional to the absolute square of the matrix element M_{if}. At smaller internuclear distances where the strong coupling regime dominates, the correlated D_2^+ wavefunction ψ_i is centered in a narrow region around the impurity atoms, and the integral range in the matrix element expression narrows, resulting in small values of the matrix element. On the other hand, when the internuclear distance is greater, the Coulomb potential has a wider internal barrier (in the $x > 0$ region), but this is not high enough to prevent the electron from passing between the donor atoms. For this reason, a significant increase in the amplitude of the matrix element occurs as a result of spreading the correlated wave function over a wider area. However, in the weak coupling regime, where the internuclear distance is sufficiently large, the internal barrier is quite wide and high such that the electron cannot easily penetrate and is therefore localizes around the donor impurity fixed at the center of the QD. Thus, the amplitude of the matrix element decreases, which leads to a reduction in the peak amplitude of the PCS.

Finally, the dependence of the PCS on QD size and internuclear distance in case II is presented in Fig. 9. Contrary to the results in case I, here the PCS amplitude increases monotonically with the parameter-D. In case II, since the donor atoms are located symmetrically on the x-axis, the internal barrier between the Coulomb centers below the base of the confinement potential $V(x, y)$ is also symmetrical. This allows the electron probability density to be centered at the center of the confinement potential. Thus, even at large D values, the electrons can be shared between donor atoms. This means that as the distance between the donor atoms increases, the correlated wavefunction ψ_i spreads over a larger region, resulting in an increase in the size of the matrix element. On the other hand, in case II as mentioned earlier, photoionization transition from the correlated ground state (initial state) to the non-correlated second excited state (final state) is allowed under the x-polarized photon field. As known the non-correlated second excited state electron wave function spreads over a larger range than that of the electron ground state wave function. As a result of this property, the size of the matrix element and the peak values of the PCS for all considered R and D values are considerably larger than the results in case I. The behavior of the spatial extension of the correlated wave function may be understood in terms of the electron cloud localization in the QD. In order to confirm the discussion above, the internuclear distance dependence of the correlated ground state wave function (initial state) is given in Fig. 10 for both cases. When the probability densities given in this figure are examined, the difference in the spatial extension of the correlated wavefunctions is clearly seen. From these results it becomes clear how the configuration of donor atoms has a significant influence on the PCS of the D_2^+ complex.

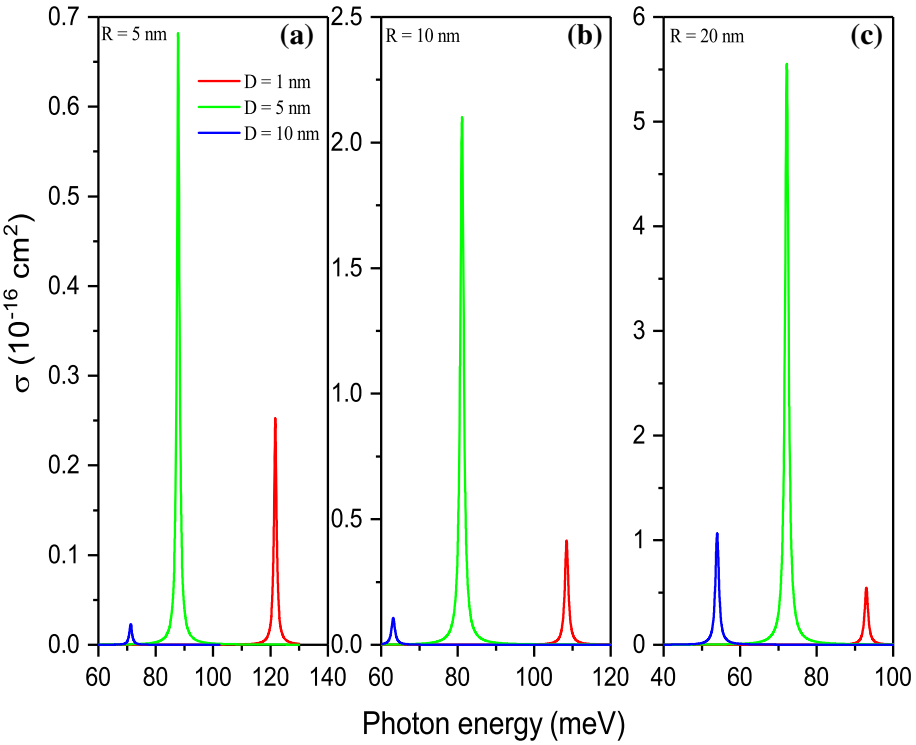

Fig. 8 PCS of the D_2^+ complex as a function of the incident photon energy for $D = 1, 5$ and $10\,nm$ when (a) $R = 5\,nm$, (b) $R = 10\,nm$, and (c) $R = 20\,nm$. Results for the case where one of the donor atoms is placed in the center of the QD

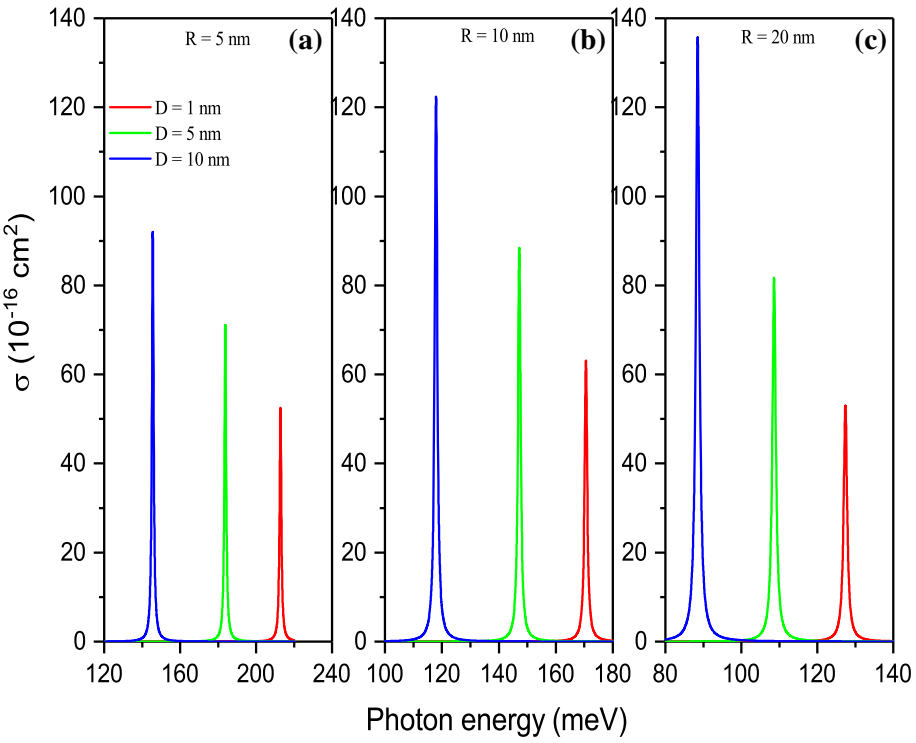

Fig. 9 PCS of the D_2^+ complex as a function of the incident photon energy for $D = 1, 5$ and $10\,nm$ when (a) $R = 5\,nm$, (b) $R = 10\,nm$, and (c) $R = 20\,nm$. Results for the case where the donor atoms are placed symmetrically on the x-axis

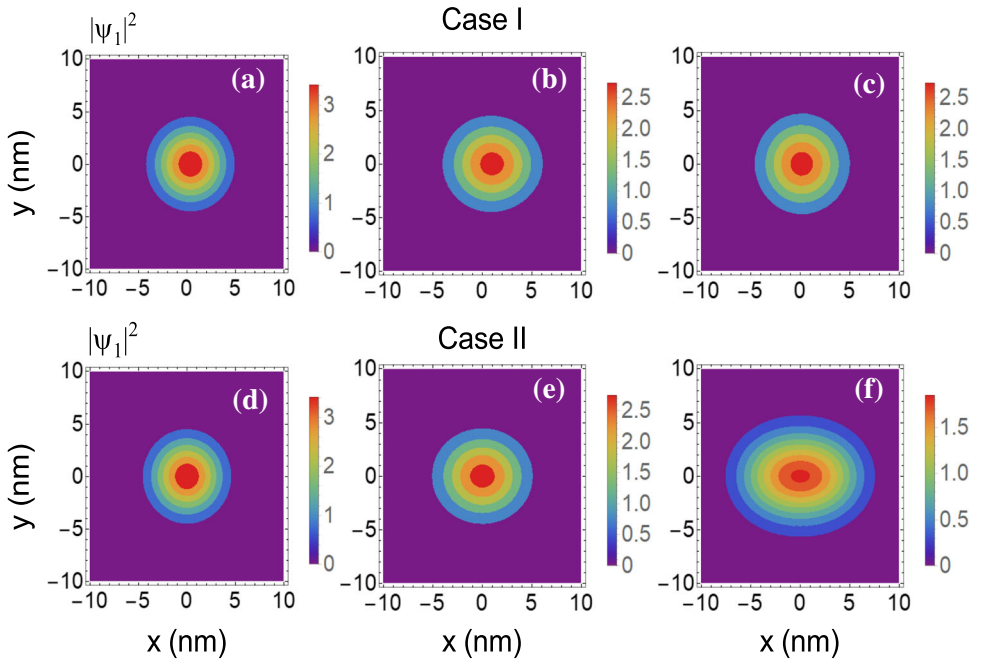

Fig. 10 Density of probability for the correlated ground state of the D_2^+ complex confined in the QD for $R = 10\ nm$. The first row is for the case where one of the donor atoms is placed in the center of the QD (case I) for (a) $D = 1\ nm$, (b) $D = 5\ nm$ and (c) $D = 10\ nm$. The second row is for the case where the donor atoms are placed symmetrically on the x-axis (case II) for (d) $D = 1\ nm$, (e) $D = 5\ nm$ and (f) $D = 10\ nm$

4 Conclusions

In this paper, we present a theoretical study on the energy spectrum, binding energy, equilibrium distance and the photoionization cross section of a singly ionized double donor complex D_2^+ confined in a quantum dot with Gaussian confinement potential. Within the framework of the effective mass approach, the energy spectrum of the D_2^+ complex was obtained numerically by using the two-dimensional diagonalization method. We conclude that the size of the quantum dot and the configuration of the donor atoms strongly affect the binding energy, equilibrium distance and photoionization cross section of the D_2^+ complex. The results show that as the effective quantum dot size gets smaller, an upward shift in total energy is observed as the position of the equilibrium distance shifts toward smaller values. Also, the dissociation energy, defined as the energy difference between the asymptotic energy for sufficiently large internuclear distance and the total energy minimum, decreases as the geometric confinement weakens. On the other hand, we have observed that when the donor atoms are very close together, the system has circular symmetry and there are doubly degenerate levels in the energy spectrum. With the increase of the distance between atoms, the circular symmetry is broken and as a result, the existing degeneration in the energy spectrum disappears. As a result, it should also be noted that the energy spectrum and optical responses of the singly ionized double donor complex can be tuned as desired by controlling the quantum dot size and impurity configuration. Also, we note that a significant increase in the amplitude of the photoionization cross section is observed when donor atoms are placed symmetrically on the x-axis. We would also like to add that the exact convergence of the results obtained in the limiting case to the known results indicates the suitability of the method used in this study.

Data Availabilty Statement This manuscript has associated data in a data repository. [Authors' comment: The data supporting this study's findings are available from the corresponding author upon reasonable request.]

Declarations

Conflict of interest The authors declare that they have no known competing financial interests or personal relationships that could have appeared to influence the work reported in this paper.

References

1. M.R. Deshpande, J.W. Sleight, M.A. Reed, R.G. Wheeler, R.J. Matyi, Spin splitting of single 0D impurity states in semiconductor heterostructure quantum wells. Phys. Rev. Lett. **76**, 1328 (1996)

2. E.E. Vdovin, Yu.N. Khanin, L. Eaves, M. Henini, G. Hill, Spin splitting of X-valley-related donor impurity states in an AlAs barrier. Phys. Rev. B **71**, 195320 (2005)
3. D. Mocatta, G. Cohen, J. Schattner, O. Millo, E. Rabani, U. Banin, Heavily doped semiconductor nanocrystal quantum dots. Science **332**, 77–81 (2011)
4. P.M. Koenraad, M.E. Flatté, Single dopants in semiconductors. Nat. Mater. **10**, 91–100 (2011)
5. D. Moraru, A. Udhiarto, M. Anwar, R. Nowak, R. Jablonski, E. Hamid, J.C. Tarido, T. Mizuno, M. Tabe, Atom devices based on single dopants in silicon nanostructures. Nanosc. Res. Lett. **6**, 479 (2011)
6. G. Long, B. Barman, S. Delikanli, Yu.T. Tsai, P. Zhang, A. Petrou, H. Zeng, Carrier-dopant exchange interactions in Mn-doped PbS colloidal quantum dots. Appl. Phys. Lett. **101**, 062410 (2012)
7. A.V. Tsukanov, Single-qubit operations in the double-donor structure driven by optical and voltage pulses. Phys. Rev. B **76**, 035328 (2007)
8. S.D. Barrett, G.J. Milburn, Measuring the decoherence rate in a semiconductor charge qubit. Phys. Rev. B **68**, 155307 (2003)
9. B. Koiller, X. Hu, S.D. Sarma, Electric-field driven donor-based charge qubits in semiconductors. Phys. Rev. B **73**, 045319 (2006)
10. J.L. Movilla, A. Ballester, J. Planelles, Coupled donors in quantum dots: quantum size and dielectric mismatch effects. Phys. Rev. B **79**, 195319 (2009)
11. S. Kang, Y.-M. Liu, T.-Y. Shi, H_2^+-like impurities confined by spherical quantum dots: a candidate for charge qubits. Commun. Theor. Phys. **50**, 767–770 (2008)
12. S. Kang, Y.-M. Liu, T.-Y. Shi, The characteristics for H_2^+-like impurities confined by spherical quantum dots. Eur. Phys. J. B **63**, 37–42 (2008)
13. R. Manjarres-García, G.E. Escorcia-Salas, I.D. Mikhailov, J. Sierra-Ortega, Singly ionized double donor complex in vertically coupled quantum dots. Nanosc. Res. Lett. **7**, 489 (2012)
14. N. Hernandez, R. Lopez, J.A. Alvarez, J.H. Marin, M.R. Fulla, H. Tobón, Optical absorption computation of a D_2^+ artificial molecule in GaAs/$Ga_{1-x}Al_x$As nanometer-scale rings. Optik **245**, 167637 (2021)
15. N. Pramjorn, A. Amthong, Donor binding energies in a curved two-dimensional electron system. Appl. Surf. Sci. **508**, 145195 (2020)
16. J.D. Salazar-Santa, D. Fonnegra-Garcia, J.H. Marin, Entropy and electronic properties of an off-axis hydrogen-like impurity in non-uniform height quantum ribbon with structural and geometrical azimuthal potential barriers. Opt. Quant. Electron. **53**, 176 (2021)
17. E. Giraldo-Tobón, J. L. Palacio, Guillermo L. Miranda, M. R. Fulla , Non-linear response under terahertz radiation of an asymmetric $Ga_{1-x}Al_xAs/GaAs/Ga_{1-y}Al_yAs$ V-groove nanowire confining a singly-ionized double donor. J. Mater. Sci. https://doi.org/10.1007/s10853-021-06738-9 (2021)
18. A. Sali, H. Satori, M. Fliyou, H. Loumrhari, The photoionization cross-section of impurities in quantum dots. Phys. Status Solidi B **232**, 209–219 (2002)
19. E. Feddi, M. El-Yadri, F. Dujardin, R.L. Restrepo, C.A. Duque, Photoionization cross section and binding energy of single dopant in hollow cylindrical core/shell quantum dot. J. Appl. Phys. **121**, 064303 (2017)
20. S. M'zerd, M. El Haouari, M. Aghoutane, M. El-Yadri, E. Feddi, F. Dujardin, I. Zorkani, A. Jorio, M. Sadoqi, G. Long, Electric field effect on the photoionization cross section of a single dopant in a strained AlAs/GaAs spherical core/shell quantum dot. J. Appl. Phys. **124**, 164303 (2018)
21. L.M. Burileanu, Photoionization cross-section of donor impurity in spherical quantum dots under electric and intense laser fields. J. Lumin. **145**, 684–689 (2014)
22. R. Arraoui, A. Sali, A. Ed-Dahmouny, M. Jaouane, A. Fakkahi, Polaronic mass and non-parabolicity effects on the photoionization cross section of an impurity in a double quantum dot. Superlattice. Microst. **159**, 107049 (2021)
23. S. Bednarek, B. Szafran, K. Lis, J. Adamowski, Modeling of electronic properties of electrostatic quantum dots. Phys. Rev. B **68**, 155333 (2003)
24. B. Szafran, S. Bednarek, J. Adamowski, Parity symmetry and energy spectrum of excitons in coupled self-assembled quantum dots. Phys. Rev. B **64**, 125301 (2001)
25. R. Khordad, Use of modified Gaussian potential to study an exciton in a spherical quantum dot. Superlattice. Microst. **54**, 7–15 (2013)
26. A. Boda, A. Chatterjee, Energy spectrum of D0 centre in a spherical Gaussian quantum dot. In: AIP Conference Proceed. **1661**, 050002 (2015)
27. R. Khordad, S. Goudarzi, H. Bahramiyan, Effect of temperature on lifetime and energy states of bound polaron in asymmetrical Gaussian quantum well. Indian J. Phys. **90**, 659–664 (2016)
28. R. Khordad Energy levels and transition frequency of strong-coupling polaron in a Gaussian quantum dot. Mod. Phys. Lett. B **28**, 1450153 (2014)
29. N. S. Yahyah, M. K. Elsaid, A. Shaer Heat capacity and entropy of Gaussian spherical quantum dot in the presence of donor impurity. J. Theor. Appl. Phys. **13**, 277-288 (2019)
30. G. Liu, R. Liu, G. Chen, Z. Zhang, K. Guo, L. Lu, Nonlinear optical rectification and electronic structure in asymmetric coupled quantum wires. Result. Phys. **17**, 103027 (2020)
31. A. Tiutiunnyka, V. Tulupenko, M.E. Mora-Ramos, E. Kasapoglu, F. Ungan, H. Sari, I. Sökmen, C.A. Duque, Electron-related optical responses in triangular quantum dots. Physica E **60**, 127–132 (2014)
32. M. Şahin, Photoionization cross section and intersublevel transitions in a one- and two-electron spherical quantum dot with a hydrogenic impurity. Phys. Rev. B **77**, 045317 (2008)
33. M. Lax, In: Proceedings of the Atlantic City Conference on Photoconductivity, Wiley, New York (1956)
34. K.F. Ilaiwi, M. Tomak, Impurity photoionization in semiconductors. J. Phys. Chem. Solid. **51**, 361–365 (1990)
35. M.I. El-Kawni, M. Tomak, Photoionization of impurities in heterojunctions. Surf. Sci. **260**, 319–322 (1992)
36. M. El-Said, M. Tomak, Photoionization of impurities in quantum wells. Solid State Comm. **82**, 721–723 (1992)
37. B. K. Ridley, Quantum Processes in Semiconductors, Oxford : Clarendon Press ; New York : Oxford University Press, 1982 **ix**, 286 (1982)
38. R.L. Greene, P. Lane, Far-infrared absorption by shallow donors in multiple-well $GaAs-Ga_{1-x}Al_xAs$ heterostructures. Phys. Rev. B **34**, 8639 (1986)
39. R. Colín-Rodríguez, C. Díaz-García, S.A. Cruz, The hydrogen molecule and the H_2^+ molecular ion inside padded prolate spheroidal cavities with arbitrary nuclear positions. J. Phys. B Atom. Mol. Opt. Phys. **44**, 241001 (2011)
40. G.M. Longo, S. Longo, D. Giordano, Spherically confined H_2^+: $^2\Sigma_g^+$ and $^2\Sigma_u^+$ states. Phys. Scripta **90**, 025403 (2015)
41. D. Skouteris, O. Gervasi A. Laganà, Non-Born-Oppenheimer MCTDH calculations on the confined H_2^+ molecular ion, Chem. Phys. Lett. **500**, 144-148 (2010)
42. I. N. Levine, Quantum Chemistry, Upper Saddle River, N.J. : Prentice Hall **5. ed**, (2000)
43. H. Sari, E. Kasapoglu, S. Sakiroglu, I. Sökmen, C.A. Duque, Impurity-related optical response in a 2D and 3D quantum dot with Gaussian confinement under intense laser field. Phil. Mag. **100**, 619–641 (2020)